Science of the Total Environment 621 (2018) 376–386

Contents lists available at ScienceDirect

Science of the Total Environment

journal homepage: www.elsevier.com/locate/scitotenv

Recent evolution of ^{129}I levels in the Nordic Seas and the North Atlantic Ocean

Carlos Vivo-Vilches [a,b,*], José María López-Gutiérrez [a,b], Raúl Periáñez [c], Charlotte Marcinko [d], Frédéric Le Moigne [e], Paul McGinnity [f,1], Juan Ignacio Peruchena [b], María Villa-Alfageme [g]

[a] Departamento de Física Aplicada I, Escuela Politécnica Superior, Universidad de Sevilla, Virgen del África 7, 41011 Seville, Spain
[b] Centro Nacional de Aceleradores (CNA) (Universidad de Sevilla, CSIC, Junta de Andalucía), Thomas Alva Edison 7, 41092 Seville, Spain
[c] Departamento de Física Aplicada I, Escuela Técnica Superior de Ingeniería Agronómica, Universidad de Sevilla, Ctra. Utrera km 1, 41013 Seville, Spain
[d] National Oceanography Centre (NOC), European Way, Southampton SO14 3ZH, United Kingdom
[e] GEOMAR, Wischhofstrasse 1-3, D-24148 Kiel, Germany
[f] Environmental Protection Agency, 3 Clonskeagh Square, Dublin 14, Ireland
[g] Departamento de Física Aplicada II, Escuela Técnica Superior de Ingeniería de Edificación, Universidad de Sevilla, Reina Mercedes 4A, 41012 Seville, Spain

HIGHLIGHTS

- Update of ^{129}I distribution in Central North Atlantic (NA) and the Nordic Seas.
- Evolution of ^{129}I from 2002 to 2012 is associated to changes in releases from NFRPs.
- Results suggest deep water formation in the eastern area of the Nordic Seas.
- ^{129}I from NFRPs partly reaches Central NA and are not carried northwards by the NCC.

GRAPHICAL ABSTRACT

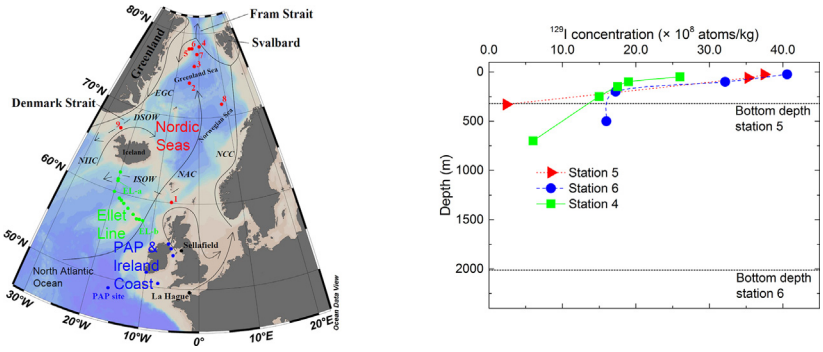

ARTICLE INFO

Article history:
Received 28 June 2017
Received in revised form 23 November 2017
Accepted 23 November 2017
Available online xxxx

Editor: D. Barcelo

Keywords:
AMS
^{129}I
Nordic Seas
North Atlantic Ocean
Deep water formation

ABSTRACT

Most of the anthropogenic radionuclide ^{129}I released to the marine environment from the nuclear fuel reprocessing plants (NFRP) at Sellafield (England) and La Hague (France) is transported to the Arctic Ocean via the North Atlantic Current and the Norwegian Coastal Current. ^{129}I concentrations in seawater provides a powerful and well-established radiotracer technique to provide information about the mechanisms which govern water mass transport in the Nordic Seas and the Arctic Ocean and is gaining importance when coupled with other tracers (e.g. CFC, ^{236}U).

In this work, ^{129}I concentrations in surface and depth profiles from the Nordic Seas and the North Atlantic (NA) Ocean collected from four different cruises between 2011 and 2012 are presented. This work allowed us to i) update information on ^{129}I concentrations in these areas, required for the accurate use of ^{129}I as a tracer of water masses; and ii) investigate the formation of deep water currents in the eastern part of the Nordic Seas, by the analysis of ^{129}I concentrations and temperature-salinity (T-S) diagrams from locations within the Greenland Sea Gyre. In the Nordic Seas, ^{129}I concentrations in seawater are of the order of 10^9 at·kg^{-1}, one or two orders of magnitude higher than those measured at the NA Ocean, not so importantly affected by the releases from the

* Corresponding author at: Centro Nacional de Aceleradores (CNA) (Universidad de Sevilla, CSIC, Junta de Andalucía), Thomas Alva Edison 7, 41092 Seville, Spain.
E-mail address: cvivo@us.es (C. Vivo-Vilches).
[1] Currently at: IAEA Environment Laboratories, 4a, Quai Antoine 1er, 98000, Monaco.

https://doi.org/10.1016/j.scitotenv.2017.11.268

NFRP. ^{129}I concentrations of the order of 10^8 atoms·kg^{-1} at the Ellet Line and the PAP suggest a direct contribution from the NFRP in the NA Ocean.
An increase in the concentrations in the Nordic Seas between 2002 and 2012 has been detected, which agrees with the temporal evolution of the ^{129}I liquid discharges from the NFRPs in years prior to this. Finally, ^{129}I profile concentrations, ^{129}I inventories and T-S diagrams suggest that deep water formation occurred in the easternmost area of the Nordic Seas during 2012.

1. Introduction

^{129}I is a long-lived radionuclide ($T_{1/2} = 15.7 \times 10^6$ years) with a strongly increasing presence in the environment since the beginning of the nuclear era. Natural processes – the cosmogenic production by spallation reactions with Xe in the atmosphere and the fission of U isotopes – result in $^{129}I/^{127}I$ atom ratios of 10^{-13} and 10^{-12} respectively (Fabryka-Martin et al., 1987). However, the anthropogenic activities (including fallout from nuclear weapons tests and discharges from nuclear power plants and, especially, nuclear fuel reprocessing plants) have resulted in $^{129}I/^{127}I$ atom ratios several orders of magnitude higher. The use of ^{129}I as an oceanographic tracer has been extensively described in previous works (Fan et al., 2013; He et al., 2013). The effectiveness of this radionuclide for such purposes is based on three important factors. Firstly, due to its long half-life, it remains in the environment for many years. Secondly, it is strongly conservative, i.e., it remains dissolved in seawater for a long time. Finally, the source terms for the main discharges of ^{129}I into the environment for the last 50 years are well documented (AREVA, 2013; López-Gutiérrez et al., 2004; Sellafield Ltd., 2014). The main releases of ^{129}I to the marine environment are liquid discharges from the two main nuclear fuel reprocessing plants (NFRP) in Europe: Sellafield (United Kingdom) and La Hague (France), which as of 2012 have released totals of 1634 kg and 4677 kg of ^{129}I respectively (Daraoui et al., 2016).

Recently, the effectiveness of ^{129}I as a radiotracer has been further enhanced because of the development of its use in combination with another long-lived radionuclide, ^{236}U, which is also released from the NFRPs. The use of $^{129}I/^{236}U$ ratio as a complementary tracer is a powerful approach for analyzing Arctic Ocean water mass behaviour in particular (Casacuberta et al., 2016; Christl et al., 2015).

The great majority of the ^{129}I discharged into the ocean has been directly released to the Irish Sea and the English Channel. Previous studies (Alfimov et al., 2006; Alfimov et al., 2004c) showed that the majority of these releases is transported through the North Sea to the Arctic Ocean along the Norwegian coast by the Norwegian Coastal Current (Villa et al., 2015). After a transit time of approximately five years in the Arctic Ocean (Orre et al., 2010; Smith et al., 2011) most of the ^{129}I is transported Southwards through the Fram Strait to the Greenland Sea (Alfimov et al., 2004c; Gómez-Guzmán et al., 2013). Furthermore, part of the ^{129}I gets involved into longer loops in the Arctic Ocean following alternative transport pathways (Karcher et al., 2012; Smith et al., 1998).

^{129}I is a particularly good tracer for circulation studies in the Arctic. e.g. Karcher et al. (2012) used model and experimental ^{129}I data from the Arctic Ocean (mid-1990s and 2000s) to illustrate the changes in oceanic circulation which occurred during that time, suggesting the development of a new Atlantic Water circulation scheme involving a separation between flow at intermediate depths in the Eurasian and Canada Basins. Orre et al. (2010) simulated ^{129}I in the North Atlantic using a OGC Model to bring insight into time-scales of tracer transport in this region were obtained. Finally, Smith et al. (2005) and Villa et al. (2015) obtained mean ages and transit times in the Nordic Seas region making use of ^{129}I concentrations.

The Nordic Seas region may crucially influence the global climate as a result of the exchange of heat that occurs between the cold Arctic Ocean and the warm North Atlantic Ocean during the formation of the deep waters in specific areas of the Nordic Seas (Open University, 2001). New data are of fundamental importance for tracing transport pathways and features of the water masses that drive the formation of North Atlantic Deep Waters (NADW). The specific location of this formation remains a topic of discussion (Hansen and Østerhus, 2000). The most recent studies support the theory that part of the NADW are formed in the eastern Nordic Seas, that is, the easternmost part of the Greenland Sea and the Norwegian Sea (Latarius and Quadfasel, 2016).

^{129}I is an ideal tracer for this purpose (Alfimov et al., 2013). The most up-to-date studies providing information on the levels of this radionuclide in the Nordic Seas and Central North Atlantic have been determined from samples collected between 2001 and 2005. Casacuberta et al. (2016) recently published updated ^{129}I concentrations for the Arctic Ocean (Canada, Makarov and Eurasian Basins). Some other studies, such as Gómez-Guzmán et al. (2013), provide updated data on levels of ^{129}I in the Irminger Basin. However, there is no up to date, comprehensive data compilation of ^{129}I concentrations either in the North Atlantic Ocean or in the Nordic Seas. This information is key for the accurate use of this radionuclide as a tracer in these areas.

In this work the distribution of ^{129}I in the Nordic Seas is analyzed, the majority of the samples analyzed are from stations located in the Norwegian Sea and the Greenland Sea. These seas connect the North Atlantic and the Arctic Oceans, thus, as previously described, they are important areas in which to monitor possible changes in the thermohaline circulation, since it is related to the North Atlantic Deep Water (NADW) formation.

The results for ^{129}I concentrations in surface seawater samples for four areas in the Nordic Seas and the North Atlantic Ocean are presented. Additionally, 11 specific depth profiles have been analyzed. The main objective of this study was to determine the current levels of ^{129}I due to NFRP discharge in these areas and to apply this data to the study of the oceanic currents. The evolution of ^{129}I concentrations in currents flowing in and out of the Nordic Seas have been analyzed and the formation of overflow waters in the Nordic Seas have been investigated through measured vertical distributions and inventories of this radionuclide.

2. Methods

2.1. Sampling

^{129}I concentrations and $^{129}I/^{127}I$ atom ratios were measured in samples from four cruises which were undertaken in 2010, 2011 and 2012 (Fig. 1).

Samples from the PAP site were sampled on board the RRS James Cook during cruise JC071 from Glasgow to the PAP site, from 29th April to 12th May 2012. The Porcupine Abyssal Plain Sustained Observatory (PAP-SO) is a multidisciplinary observatory in the North Atlantic. These samples were collected in one of the regular cruises that take place to the site to collect equipment time series datasets. Samples at the Ellet line were sampled on board RRS Discovery (cruise D379 in August 2012). The Ellet Line is a route of long term oceanographic observations that links Scotland and Iceland through the Rockall Plateau and the Iceland Basin, separating the Nordic Seas from the North Atlantic. During the Ellet cruises, regular samplings are made to assess climate stability.

Greenland, Norwegian and Barents Seas were sampled on board James Clark Ross (British Antarctic Survey) during the UK's Ocean Acidification program, from 12th June to 1st July 2012.

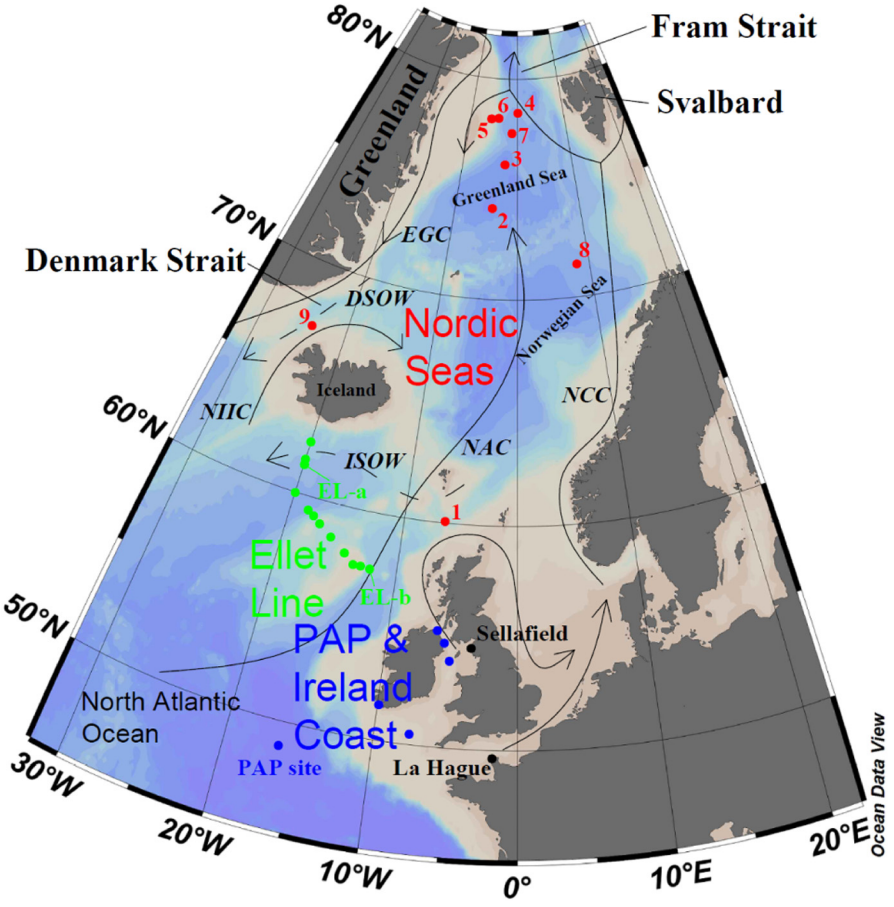

Fig. 1. Sampling sites and currents involved in the ^{129}I transport to the different regions of the Nordic Seas and the Arctic Ocean, as well as locations of Sellafield and La Hague NFRPs. NCC stands for Norwegian Coastal Current; NAC, for North Atlantic Current; EGC, for East Greenland Current; NIIC, for North Icelandic Irminger Current; DSOW, for Denmark Strait Overflow Water; and ISOW, for Iceland Scotland Overflow Water. These two last water masses are represented with dash lines to represent that they are deep water masses.

Surface samples from the Ireland Coast were sampled between 25th April and 10th December 2010 and between 22nd and 30th July 2011 by the Irish Environmental Protection Agency.

For the cruises, in all cases discrete water samples were collected using a stainless steel sampling rosette equipped with 24 × 20 L Niskin® bottles and a CTD Seabird® sensor package. When a depth profile was collected, it was designed to have greater resolution in the upper 500 m. Deeper samples were collected according to the needs of the cruise and prior knowledge of the distribution of water masses. Water samples were transferred into polyethylene bottles, firmly sealed and stored in a cold dark room.

2.2. Sample preparation and measurement

The method adopted in this work for the chemical preparation of seawater samples has been described previously by López-Gutiérrez et al. (2000) for fresh waters. In summary, the volume of water used was selected depending on the expected ^{129}I concentration and on the available amount of sample available. The volumes collected ranged from approximately 100 to 600 ml. Woodward Iodine (2 mg) was added to the sample as a carrier. By the addition of $NaHSO_3$, all iodine species were reduced to I^- and afterwards oxidized to I by the addition of HNO_3 and $NaNO_2$. In these conditions, I was extracted into $CHCl_3$ and then back-extracted into aqueous solution by $NaHSO_3$ again. This step was repeated three times in order to purify I in the sample. Finally, $AgNO_3$ was used to precipitate iodine as AgI, mixed with Nb powder and pressed into a Cu cathode for the AMS measurement. Blank samples were prepared from double distilled water in the same way as real samples. All these values included correction by the instrumental blank ratio of the system, obtained by the measurement of unprocessed Woodward Iodine.

Measurements were carried out at the 1 MV AMS facility at the Centro Nacional de Aceleradores in Sevilla (CNA, Spain). The measurement method has been previously described in detail (Gómez-Guzmán et al., 2012). In brief: I^- is measured with characteristic currents at the low energy side are between 1 and 5 μA. The terminal voltage is 1 MV and the selected charge state is 3+, for which transmission in the Ar stripper is approximately 9%. Measured atom ratios are corrected by an internal standard, whose nominal ratio is $^{129}I/^{127}I = (4.664 \pm 0.20) \times 10^{-11}$.

In order to validate the preparation and measurement methods, several certified reference materials have been analyzed with results in agreement with certified values: IAEA-418 (Pham et al., 2010), IAEA-381, IAEA-375 and IAEA-414.

The measured atom ratio strongly depended on the location from which the sample was collected. For Nordic Seas samples, $^{129}I/^{127}I$ atom ratios of an order of 10^{-11} were measured, for Ellet samples ratios were typically between 5×10^{-12} and $1 \times 10^{-11}$and for PAP samples they were between 5×10^{-13} and 1×10^{-12}. Average atom ratios for chemical blanks were around 1×10^{-13} in all cases.

3. Results and discussion

3.1. Description of ^{129}I sources and regional oceanography in the Nordic Seas

Fig. 1 shows the location of the stations, as well as the main currents in the Nordic Seas, which transport ^{129}I from the locations of its liquid and gaseous discharges (Sellafield and La Hague) to the different areas

of the North Atlantic and the Arctic Oceans (He et al., 2013). Liquid discharges are released directly to the Irish Sea, in the case of Sellafield; and to the English Channel, in the case of La Hague. Annual liquid discharges of ^{129}I released between 1986 and 2012 from these two plants are shown in Fig. 2. Note that in 1994 releases significantly increased and they reached a maximum in 1998, just after the start of the operation of the Thermal Oxide Reprocessing Plant (THORP) plant, in 1994, in Sellafield; and the start of operation of the UP3 plant and upgrade of the UP2 plant, in 1990 and 1994 respectively, in La Hague (IAEA, 2005). Most of this ^{129}I is carried northwards along the Norwegian Coast by the Norwegian Coastal Current (NCC); but in recently published models it is also shown that part of those discharges could be transported south-west and have a direct impact in the Atlantic Ocean (Orre et al., 2010; Villa et al., 2015).

While NCC is colder and less salty than North Atlantic Water (NAW) it is considerably warmer and saltier than the Arctic waters. After reaching Svalbard Archipelago, the NCC containing dissolved ^{129}I splits into two currents: one travels in the direction of the Greenland Sea, and the other to the Arctic Ocean through the Fram Strait. The water which enters the Arctic Ocean will eventually return to the Fram Strait, and will exit from the Arctic Ocean close to the East Greenland Coast.

The left branch of the NAW surface current turns westward, forming the anticlockwise subpolar gyre and flows around the southwest shelf of Iceland (Holliday et al., 2006; Rhein et al., 2011). This current flows north around the north of Iceland, and is named the North Icelandic Irminger Current (NIIC). It collides with the Modified East Icelandic Water (MEIW), an eastward branch of the East Greenland Current (EGC) (Logemann and Harms, 2006; Waite et al., 2006).

The EGC is formed by water coming out of the Arctic Ocean through the Fram Strait that mixes with water coming directly from Svalbard Archipelago to the East Greenland Coast. This corresponds to the turnover of the NAC in the Nordic Seas, also fed by the contribution of the left branch of the NCC. The EGC carries a large amount of low-density and cold surface Arctic waters and denser and warmer intermediate Atlantic waters southward along the edge of the Greenland continental shelf (Fogelqvist et al., 2003; Lacan and Jeandel, 2004; Waite et al., 2006).

The EGC transports ^{129}I southbound from the Fram Strait along the Greenland Coast to the Denmark Strait, where it finally leaves the Nordic Seas. At that point, the EGC joins the NIIC, which flows in the opposite direction, as described above.

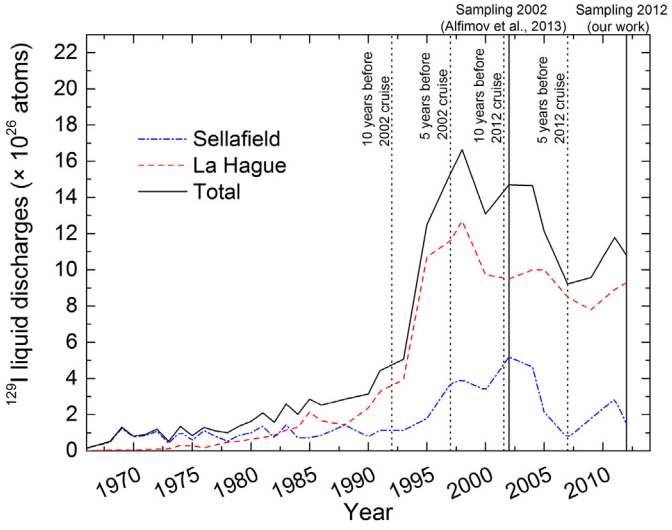

Fig. 2. Annual ^{129}I liquid discharges from the Nuclear Fuel Reprocessing Plants of Sellafield and La Hague from 1986 to 2012. In the late 90's, these discharges reached their maximum. The sampling years of both cruise are presented (2002 and 2012). We also mark the year when discharges started to increase significantly (1993), the year of the maximum release (1998) and a relative minimum in these releases in 2007.

All of these processes are connected to the NADW, a deep water mass that is formed in the North Atlantic Ocean and is closely tied to the thermohaline circulation of the World Ocean. NADW includes the Labrador Sea Water and the Nordic Sea Overflow Water (NSOW).

While surface water enters the Nordic Seas from the North Atlantic with the NAC, the deep NSOW water outflows from the Nordic Seas across the Greenland-Scotland Ridge (Dickson and Brown, 1994) forming two overflow waters that outflow southward: the DSOW (Denmark Strait Overflow Water), between Greenland and Iceland, as part of the East Greenland Current (Jeansson et al., 2008); and the ISOW (Iceland-Scotland Overflow Water), between Iceland and Scotland (Hansen and Østerhus, 2000). These two water masses meet in the Irminger Basin (Tanhua et al., 2005).

NSOW is formed in the Nordic Seas to intermediate depths (Bacon, 1998), and is colder and saltier than water from the Labrador Sea. Hence it is the densest water of the NADW (Dickson and Brown, 1994; Smethie et al., 2000). Several mechanisms contribute to the production of these deep water masses, i) the input of low-salinity surface waters from the Arctic Ocean, which remain at the surface level and force other water masses to sink (Alfimov et al., 2004a); ii) open ocean convection in the waters flowing northwards, by the formation of colder, more saline and, hence, denser waters, mainly due to rapid evaporation in the surface layers due to the strong Arctic winds.

3.2. Nordic Seas: time and geographical evolution of ^{129}I concentrations and Deep Water Formation

Measured ^{129}I surface concentrations close to the Norwegian Coast reached levels as high as 10^{10} atoms·kg^{-1} in the late 1990s (Alfimov et al., 2013; Alfimov et al., 2004b; Michel et al., 2012). These concentrations were at least three order of magnitude than the nuclear weapons test fallout background in the North Atlantic, which has been estimated to be 2.5×10^7 atoms·kg^{-1} (Fehn et al., 1986). Furthermore, they are one order of magnitude higher than those measured in the same area during the late 1970s, which were lower than 10^9 atoms·kg^{-1} (Edmonds et al., 1998).

The temporal evolution of ^{129}I concentrations in some locations from the Arctic Ocean demonstrated an appreciable elevation five years after the increase in ^{129}I liquid discharges from NFRPs in 1994 (Smith et al., 2011). This was detected in locations close to the Fram Strait, where water currents enter the Arctic Ocean. Likewise, 10 years after the NFRP discharges increased, elevated ^{129}I concentrations were detected at locations coincident with Arctic Ocean outflow to the Fram Strait (Smith et al., 2011).

Thus, in 1996 ^{129}I surface concentrations in the Arctic Ocean were of the order of 10^8 atoms·kg^{-1} (Buraglio et al., 1999), and in 2001 they had increased to around 1.8×10^9 atoms·kg^{-1} (Alfimov et al., 2004b).

Water flowing out of the Arctic Ocean through the Fram Strait carrying ^{129}I input into the Arctic Ocean from the right branch of the NCC is mixed with water from the turnover of the NAC in the Nordic Seas, itself fed by ^{129}I from the left branch of the NCC. Surface concentrations at location in the Fram Strait closest to Greenland increased from 1×10^9 atoms·kg^{-1} in 2002 (Alfimov et al., 2013) to 5×10^9 atoms·kg^{-1} in 2005 (Michel et al., 2012). Interestingly, in locations closer to Svalbard, concentrations remained at almost constant levels slightly higher than 2×10^9 atoms·kg^{-1} during those years.

The stations in the Nordic Seas from which samples were collected for this work are shown in Fig. 3. This map also includes stations from which samples were collected during a 2002 cruise that (Alfimov et al., 2013), which are located very close to those investigated in this study. Comparison with the results from 2002 and with the temporal evolution of the discharges from NFRPs, facilitates interpretation of the temporal evolution of ^{129}I concentrations in this area.

Table 1 shows that the highest ^{129}I concentrations are those from the stations 2–7, located in the Greenland Sea. Notably, the surface levels from stations 6, close to the Greenland Coast, and station 5, in the border

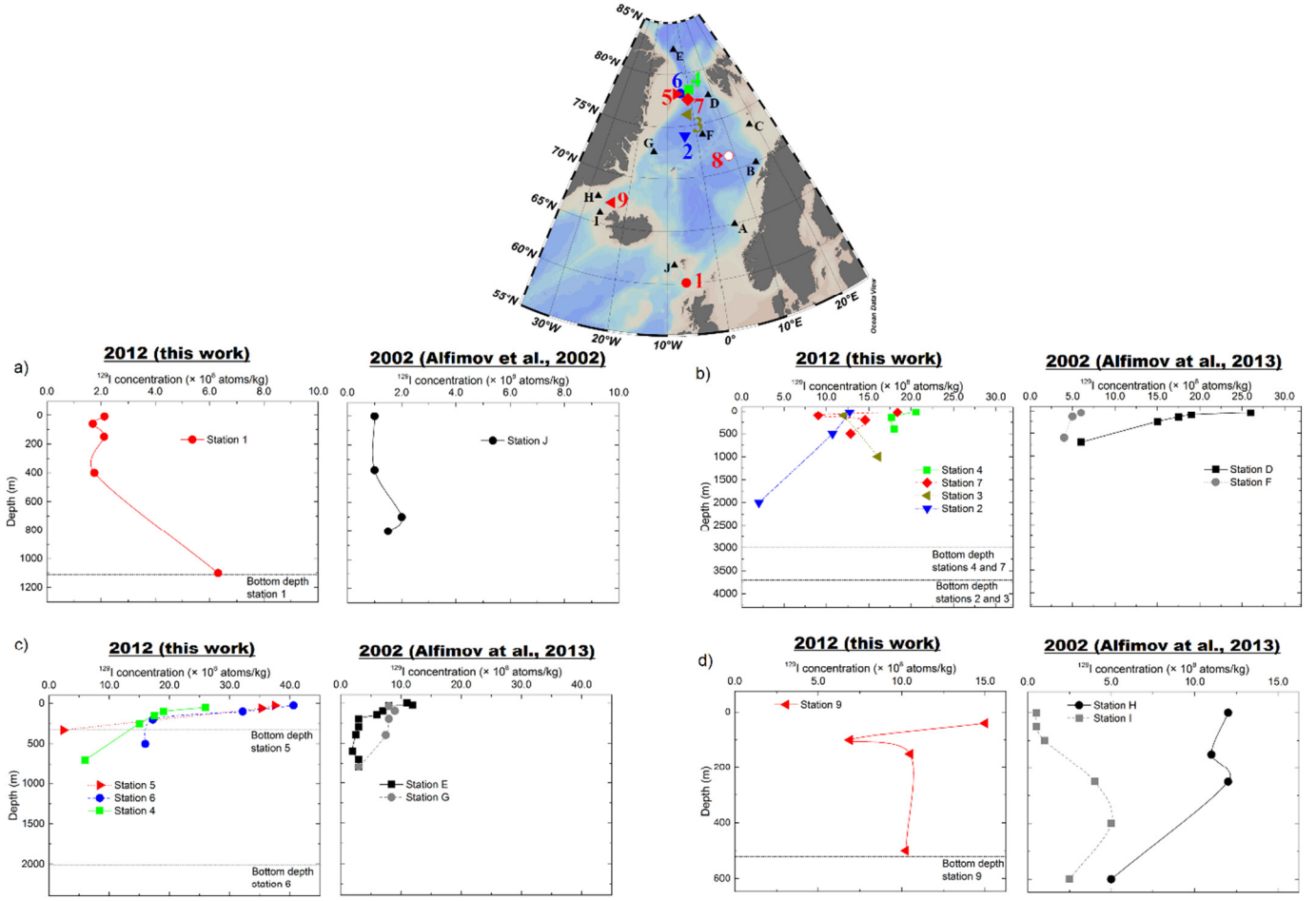

Fig. 3. Sampling locations in the Nordic Seas from this work, in different colors; from Alfimov et al. (2013), in black, but changing the numbers of the stations to letters to avoid confusing with our stations. ^{129}I concentration depth profiles are also shown: a) Faroe Bank Channel; b) Greenland Sea; c) East Greenland Coast; d) Denmark Strait.

of the continental platform (330 m depth for station 5), were found to be up to approximately two times higher than those from the open ocean areas of the Greenland Sea (stations 2, 3, 4 and 7).

The lowest ^{129}I concentration found, at station 1 close to the Faroe Islands, is one order of magnitude lower than those from the other stations in the Nordic Seas. The surface ^{129}I concentration in this station was found to be 2.1×10^8 atoms·kg^{-1}, double the level measured in 2002. An even larger difference is found below 500 m, where the ^{129}I concentration measured was 6.3×10^8 atoms·kg^{-1}, while in 2002 levels were close to 2×10^8 atoms·kg^{-1}.

Most of the samples analyzed in the Nordic Seas present lower concentrations in 2002 than in 2012. The high concentrations – up to 10^{10} atoms·kg^{-1} at station B from the 2002 cruise –therefore probably reflect the ^{129}I maximum that took place in 1998. Higher concentrations – up to 2.5×10^9 atoms·kg^{-1} – were also measured in 2002 at station D close to the entrance of Svalbard, corresponding to water masses directly from the NCC entering into the Arctic Ocean through the Fram Strait. These high concentrations were related to the previous increase in ^{129}I releases in 1994, already in the 10^{27} atoms·year^{-1} level. Precisely in 1997, five years before sampling D station in 2002, there was a maximum in the releases (see more details in Fig. 2).

In contrast, station F from the 2002 cruise, located very close to station D, presents concentrations lower than 10^9 atoms·kg^{-1}, almost one order of magnitude lower than station D and lower that 2012. This station receives only a part of the ^{129}I initially carried by the NCC since it is in the inner part of the Norwegian Sea and, additionally, is mixed with the uncontaminated NAC, which flows northwards between the British Isles and Iceland with a contribution of the NFRPs whose ^{129}I concentrations are orders of magnitude below those from the NCC.

With exceptions, Fig. 3 shows that stations 2, 3, 4, 7 and 9 generally higher ^{129}I concentrations were measured in 2012 than in 2002.

The measured ^{129}I concentration in surface water from station 8 is also especially low. The origin of the water masses in this area is warm, low salinity water from the NAC not directly influenced to Sellafield and La Hague.

The ^{129}I sub-surface concentrations from station 8 are similar to those measured in the Greenland Sea. Indeed, it is known (Open University, 2001) that deep water formed in the Greenland Sea may spread and accumulate in the Norwegian Sea. The similar ^{129}I concentrations may be indicative of this process.

Salinity and temperature in the samples from the 2012 cruise were measured for depths down to 500 m. Salinity-temperature diagrams, which can be seen in Fig. 4, allow an initial interpretation of the origin of the water masses.

There is an increase in surface water temperature at stations 2, 3, 7 and 4 in a northwards direction. The coldest surface water is found at station 2, which is in the area of the Greenland Gyre. Water in the gyre above 1500 m is between −1.1 and −1.7 °C (Pickard and Emery, 1982). This water is colder than water in the Arctic Ocean at the same depth. North of this station, incoming NCC water leads to an increase in surface water temperature. An Arctic influence is apparent deeper in the water column, as indicated by the temperature decrease.

Table 1
^{129}I concentrations in different sampling positions in the Nordic Seas.

Sampling region	Station	Latitude (°N)	Longitude (°E)	Bottom depth (m)	Depth (m)	^{129}I concentration (10^8 atoms·kg^{-1})	3σ (10^8 atoms·kg^{-1})
Faroe Bank	1	60.08	−6.42	1110	10	2.12	0.19
					60	1.69	0.37
					150	2.11	0.05
					400	1.75	0.07
					1100	6.31	0.08
Norwegian Sea	8	71.44	8.26	1770	20	1.28	0.57
					100	13.18	0.34
					200	14.58	0.41
					500	11.59	0.86
Greenland Sea	4	78.43	0	2850	20	20.58	0.40
					150	17.70	0.84
					400	18.01	0.49
	7	77.51	−1.15	3080	25	18.38	0.40
					100	9.03	0.19
					200	14.56	0.65
					500	12.85	0.38
	3	76.10	−2.32	3720	100	12.08	0.32
					1000	16.08	0.25
	2	74.06	−4.11	3620	20	12.74	0.53
					500	10.72	0.24
					2000	2.03	0.18
East Greenland Coast	5	78.12	−5.59	340	25	37.5	1.5
					60	35.3	1.6
					330	2.36	0.32
	6	78.17	−4.14	2010	25	40.6	1.7
					100	32.2	1.3
					200	17.24	0.55
					500	15.99	0.33
Denmark Strait	9	67.16	−24.04	520	40	14.99	0.57
					100	6.89	0.34
					150	10.50	0.41
					500	10.25	0.86

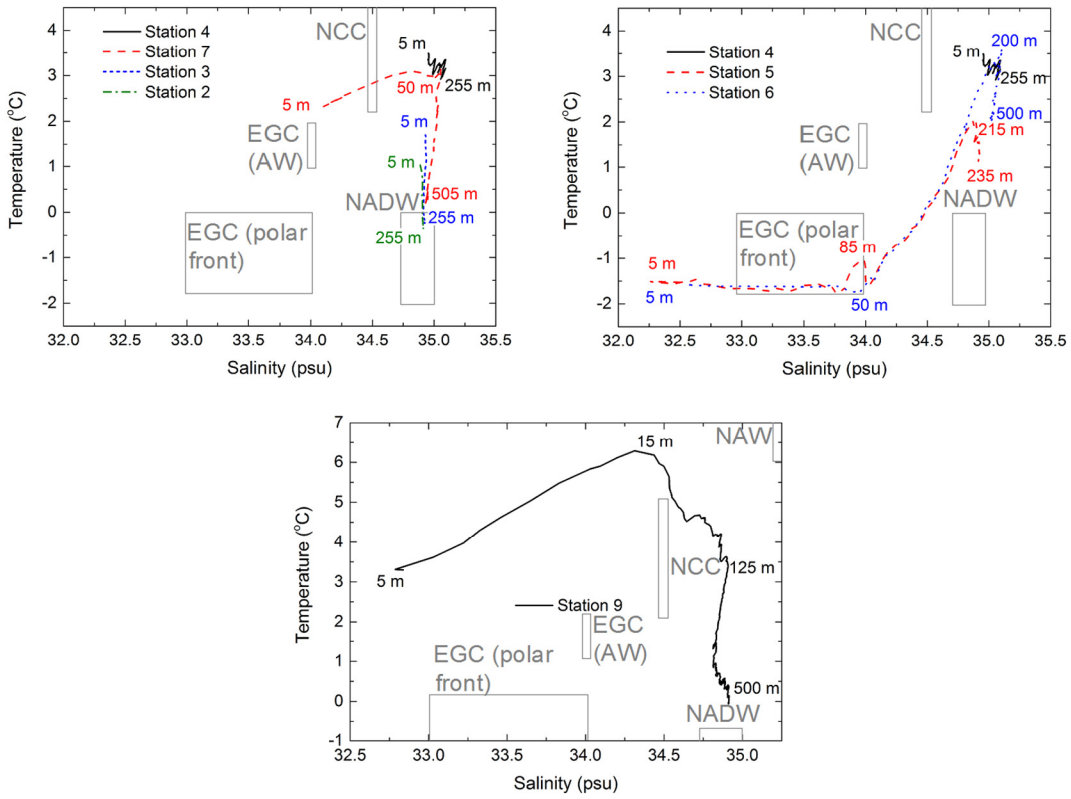

Fig. 4. Salinity-temperature diagrams for the stations located in the Greenland Sea (up, left), the East Greenland Coast (up, right), and the Denmark Strait (down). Temperature and salinity ranges from main water masses in the area are also shown: Norwegian Coastal Current (NCC), North Atlantic Water (NAW), East Greenland Current (EGC), and North Atlantic Deep Water (NADW). These diagrams, together with ^{129}I concentration depth profiles, can help us assess the origin of each water mass. No data from waters deeper than 500 m are available.

Accordingly, an increasing trend with latitude in ^{129}I concentrations is observed at the stations in the Greenland Sea that follow the NAC current up to the Fram Strait (2, 3, 7 and 4). The surface levels of ^{129}I concentrations, from south to north, are: 1.274×10^9 atoms·kg^{-1} at station 2 (74.06°N), 1.208×10^9 atoms·kg^{-1} at station 3 (76.10°N), 1.838×10^9 atoms·kg^{-1}at station 7 (77.51°N), and 2.058×10^9 atoms·kg^{-1} at station 4 (78.48°N). The high ^{129}I concentrations detected at stations 4 and 7 are thus due to water originating from the NCC, carrying high ^{129}I concentrations directly from the reprocessing facilities (He et al., 2013) and likely correspond to water masses which inflow the Arctic Ocean with high salinity and temperatures above 0 °C. Note that, although the surface level at station 3 is slightly lower than at station 2, this may be because the first sample for station 3 was collected at a depth of 100 m, while for station 2 it was 20 m.

In contrast, surface water from stations 5 and 6, in the East Greenland Coast, correspond mainly to Polar Water which outflows from the Arctic Ocean to form the East Greenland Coastal Current. These stations are located on both sides of the continental slope, along the pathway of the EGC, coming from the Arctic Ocean. This is confirmed by the T-S diagram showing low salinity and temperatures below 0 °C. In these stations Surface Arctic Water is found in the first 50–100 m, with a salinity between 28 and 33.5 and a temperature around −1.5 °C (Pickard and Emery, 1982).

The highest ^{129}I concentrations are found in the surface samples at these stations with concentrations at the $3–4 \times 10^9$ atoms·kg^{-1} level. This is because water at stations 5 and 6 outflows from the Arctic Ocean and the transit time from the NFRPs out of the Arctic is approximately 13–14 years. Thus this water carries ^{129}I released in 1998 when the NFRPs releases were at a maximum (see more details in Fig. 2). In contrast, stations 4 and 7, with waters that inflow into the Arctic, probably detect ^{129}I carried from the relative minimum in the NFRPs releases in 2007.

For stations 5 and 6, surface levels of ^{129}I were also found to be higher in 2012 than in 2002: around 4×10^9 atoms·kg^{-1} in 2012 compared to 1.25×10^9 atoms·kg^{-1} in 2002. ^{129}I concentration in surface water from station 9 (also in the pathway of the EGC) is 1.499×10^9 atoms·kg^{-1}, lower than at stations 5 and 6, indicating some mixture with North Atlantic Central Water, with a lower content of ^{129}I.

Both stations present similar ^{129}I concentrations, salinity and temperature for surface water. This means that surface water from both points has the same origin. However there is an obvious difference between stations 5 and 6 below 200 m, since station 5 is at the border of the continental platform (330 m depth), whereas Station 6 is a deeper site (2010 m). Below 200 m, ^{129}I concentration at station 6 (1.599×10^9 atoms·kg^{-1}) is an order of magnitude higher than at station 5 (2.36×10^8 atoms·kg^{-1}).

At depths further down the water column at station 6, between 200 and 300 m, Atlantic Water with ^{129}I concentration lower than 2×10^9 atoms·kg^{-1} is detected, with a salinity of approximately 34.8 psu, and temperature between 0 and 3 °C (Pickard and Emery, 1982). The Atlantic Water eroded core is apparent at 200 m depth, in agreement with previous data (Pickard and Emery, 1982), more significantly at station 6, with temperatures higher than 2 °C at a depth of 200 m. Below 200 m, water temperature continues decreasing in the water column in both stations due to mixing with the Arctic Bottom Water, which is colder.

As explained above, the T-S diagram from station 6 clearly shows two different water masses which mix between 100 m and 200 m depth: surface waters present low salinities (from 32 to 34 psu) and temperatures below 0 °C typical from Arctic surface waters (Buraglio et al., 1999). At 200 m, the ^{129}I concentration is around 1.7×10^9 atoms·kg^{-1} at station 6, as well as at station 4, closer to Svalbard (see Fig. 3). Salinity and temperature at station 4 are also equal to those at 200 m depth at station 6 (see Fig. 4), showing that ^{129}I values probably correspond to the same water mass.

Finally, the ^{129}I concentration at station 9, in the Denmark Strait, decreases from 1.499×10^9 atoms·kg^{-1}at a depth of 40 m to 6.89×10^8 atoms·kg^{-1}at 100 m, and increases to levels close to 1×10^9 atoms·kg^{-1}for waters deeper than 150 m.

Three water types seem to be present at sampling station 9, which is also under the influence of the EGC, traveling between Iceland and Greenland. First, the surface water with low salinity and high temperature is probably due to some mixture of North Atlantic Central Water (temperature around 9 °C) and North Icelandic Irminger Current (NIIC) (Open University, 2001). Deeper in the water column, properties are closer to those of the NADW, with a higher salinity, close to 35 psu (Open University, 2001).

The results from Smith et al. (2011) correspond mainly to the Irminger Basin, but there is a station in the Denmark Strait which can be compared to the results from station 9 (Fig. 3). The surface ^{129}I concentration at that station, which is 1.499×10^9 atoms·kg^{-1}, is 2.5 times higher than in the Strait in 1999, while only 1.25 times higher than in 2002 in the station H (Alfimov et al., 2013). This agrees with our previous hypothesis showing that surface ^{129}I concentrations at stations 5 and 6 in 2012 were influenced by the 1998 maximum in ^{129}I liquid discharges. The surface ^{129}I concentration at station 9, in the Denmark Strait, is much lower than at stations 5 and 6, from the Nordic Seas, because it mixes with the North Atlantic Central Water which has much lower levels of ^{129}I.

In relation to the formation of the North Atlantic Deep Waters, at station 6, waters below 200 m depth present salinities higher than 35 psu, temperatures above 0 °C and higher ^{129}I concentrations. This probably correspond to the DSOW flowing southbound, produced in the Greenland Sea at stations 3, 4 and 7. Furthermore, the incoming of low-density Arctic Ocean water from the Fram Strait also contributes sinking of the dense water originating in the Greenland Sea (Huang, 2010; Open University, 2001).

In Fig. 5 we present ^{129}I inventories, estimated using a simple rectangle method to integrate the ^{129}I concentration. Note that, to obtain the maximum accuracy using this method, we need high resolution profiles to cover all data points from shallow to deep waters. However, some of the depth profiles were not extensively sampled with depth meaning that some profiles present a relatively high uncertainty in their inventories. To estimate this uncertainty, the inverse of the square root of the number of samples from that depth profile was used. The highest inventories are found in the Norwegian Sea and the East area of the Greenland Sea, where they reach levels 10 times higher than, for instance, that from station 1, close to the Faeroe Islands.

Arctic surface waters are an additional factor contributing to the higher fraction of ^{129}I inventories in the upper 200 m for stations 6

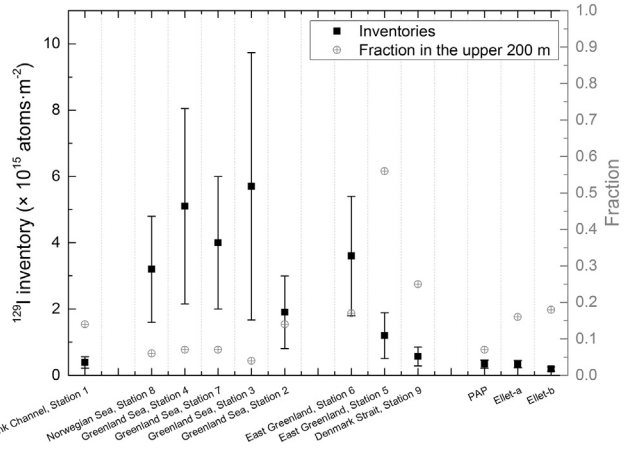

Fig. 5. ^{129}I inventories in some of the stations in this work. In grey, the fraction of that inventory coming from the upper 200 m.

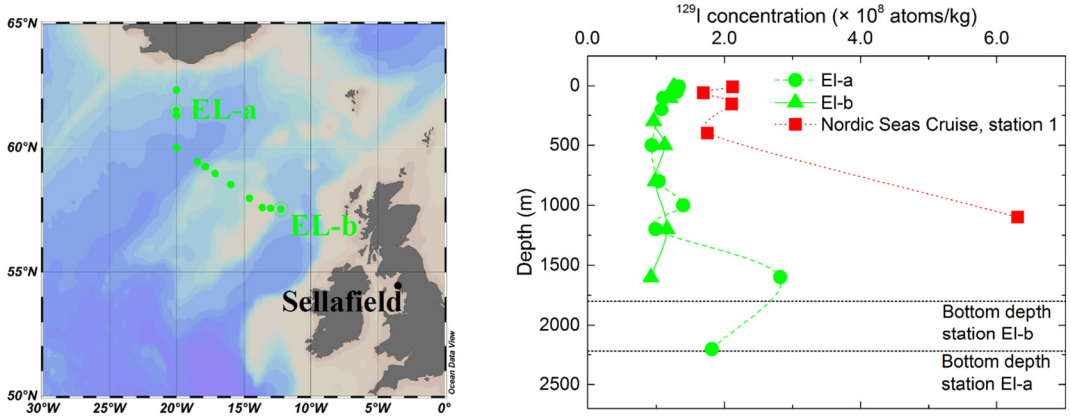

Fig. 6. Sampling locations in the Ellet Line and ^{129}I concentration depth profiles of two of them. Main difference between both can be seen for deep layers, where ^{129}I concentration is much higher in the station closer to Iceland.

(17%) in contrast with those for stations 4, 7 and 3, where this fraction is significantly lower than 10%. Note that, as described above, in 2012 water transported from the Arctic Ocean to the Greenland Sea forming the shallow current flowing southbound (Open University, 2001) along the East Greenland Coast probably transported high ^{129}I concentrations associated with the maximum ^{129}I liquid discharges from 1998.

The ^{129}I concentrations at stations 2 and 3, between 20 and 500 m depth, are similar to those of station 9 below 150 m and to 500 m and are approximately 1×10^9 atoms·kg^{-1}. The similar T-S properties (high salinity and temperature between 0 °C and 3 °C) and similar ^{129}I concentrations in these stations suggest that deep water is being effectively formed in the area of the Greenland Sea in the vicinities of stations 2 and 3, and that this water is overflowing through the Denmark Strait (station 9). The ^{129}I concentration and T-S properties at station 6 for waters deeper than 200 m are also similar, reinforcing this theory.

As we described above, the origin of the deep waters in the Nordic Seas was traditionally associated with western locations of the Greenland Sea. However, the exact location of the formation has been queried in recent years. It has been found that the eastern Nordic Seas may also play an important role in the formation of the NSOW (see, for example, Latarius and Quadfasel, 2016 and references therein).

^{129}I inventories in the Nordic Seas, presented in Fig. 5, can be used as a complementary approach to T-S diagrams to estimate the origin of the NADW. Stations 3, 4 and 7, in the Greenland Sea, and station 8, in the Norwegian Sea, have the highest total ^{129}I inventories. Most of the ^{129}I content in these stations comes from the deeper layers, since the fraction of ^{129}I from the upper 200 m is less than 10%. The highest inventories at stations 3, 4, 7 and 8, combined with the low fraction of the inventories in the upper 200 m, may be due to the sinking of surface waters, enriched in ^{129}I from the NCC, to the bottom depths. However, better resolution profiles would be needed to facilitate a more definitive comparison of inventories.

The results of this work, including ^{129}I concentrations, inventories and T-S diagrams, indicate that the sampled area including stations 3, 4, 7 and 8 could be areas of deep water formation; the DSOW in the Greenland Sea, in the case of stations 4, 7 and 3; and the ISOW in the Norwegian Sea, in the case of station 8 (see Section 3.1). This confirms that part of the formation of deep waters in the Nordic Seas was located in the eastern part of the Nordic Seas in 2012.

According to Latarius and Quadfasel (2016), the formation of the deep waters that later conform the Denmark Strait Overflow Water and the Iceland-Scotland Overflow Water covered a vast area from latitudes 71°N (Station 8) to 79°N (Station 4) and from longitudes 2.3°W (Station 3) to 8.30°E (Station 8). The results from this work complement and support these conclusions.

3.3. NFRPs contribution to ^{129}I concentrations in the North Atlantic Ocean

Two different sets of locations in the North Atlantic Ocean have been studied: one in the Ellet Line, and a second one on the Irish Coast and the Porcupine Abyssal Plane (PAP).

Surface levels of ^{129}I concentrations were measured in the sampling locations shown in Fig. 6; additionally, there are depth profiles from 2 stations: one closer to Iceland, denoted as El-a; the other one closer to the British Isles, denoted as El-b. Results for Ellet Line stations are presented in Table 2. ^{129}I concentrations are typically at the 10^8 atoms·kg^{-1} levels. These values are clearly lower than the ones in the Nordic Seas, as expected, since the influence of Sellafield and La Hague should decrease to the west.

Both depth profiles, from stations El-a and El-b, presented in Fig. 6, show similar behaviour for waters up to 1200 m depth, and ^{129}I

Table 2
^{129}I concentrations in the Ellet Line.

Station	Latitude (°N)	Longitude (°E)	Bottom depth (m)	Depth (m)	^{129}I concentration (10^8 atoms·kg^{-1})	3σ (10^8 atoms·kg^{-1})
El-b	57.51	−12.25	1800	8	1.266	0.020
				16	1.243	0.065
				50	1.232	0.041
				100	1.199	0.057
				300	0.960	0.068
				500	1.121	0.046
				800	0.985	0.047
				1200	1.16	0.16
				1600	0.920	0.073
	57.55	−13.00		5	1.451	0.069
	57.58	−13.63		7	1.035	0.059
	57.95	−14.59		5	1.647	0.079
	58.50	−16.00		5	1.262	0.084
	58.95	−17.18		5	1.498	0.059
	59.21	−17.88		5	1.419	0.028
	59.40	−18.42		5	1.479	0.096
	60.00	−20.00		8	1.82	0.12
	61.26	−20.00		5	1.74	0.12
El-a	61.50	−20.01	2220	5	1.331	0.045
				50	1.299	0.058
				100	1.101	0.077
				200	1.074	0.065
				500	0.933	0.028
				800	1.034	0.069
				1000	1.395	0.084
				1200	0.986	0.059
				1600	2.82	0.17
				2206	1.816	0.071
	62.33	−19.84		5	2.05	0.24

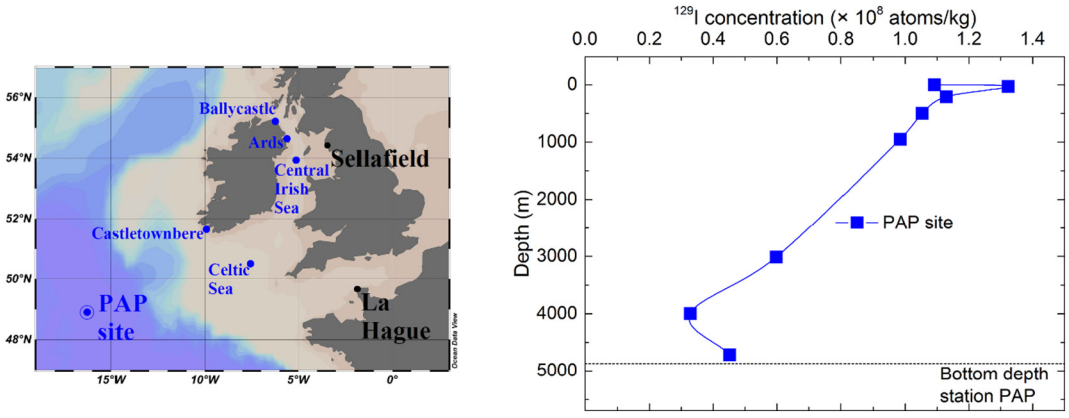

Fig. 7. Sampling locations in the Irish and Celtic Seas, and the Porcupine Abyssal Plain, from which the ^{129}I concentration is shown. Surface concentration is much higher than the one coming from fallout.

concentration remains almost constant (around 1×10^8 atoms·kg^{-1}). However, at waters deeper than 1200 m, ^{129}I concentration almost triples surface level in the profile close to Iceland because of the ^{129}I transported back from the Norwegian Sea by the intermediate ISOW, while it remains constant in the profile closer to the British Isles.

The second set of sampling locations, in the Ireland Coast and the PAP, is used to study the possible direct impact in the North Atlantic Ocean of Sellafield and La Hague. These locations are shown in Fig. 7. ^{129}I concentrations, which are shown in Table 3, are obviously much higher in the Irish Sea, where they reach 1.58×10^{11} atoms·kg^{-1} (Ards Station), due to the direct releases from Sellafield. In the Celtic Sea, surface ^{129}I concentration is lower – 7.65×10^8 atoms·kg^{-1} – while at the PAP site it is lower still, around 10^8 atoms·kg^{-1}.

Low concentrations at the PAP site are expected because most of the liquid discharges from Sellafield and La Hague are advected directly to the Nordic Seas by the NCC (Alfimov et al., 2004a). However, concentrations are four times higher than estimated ^{129}I background concentrations in the North Atlantic Ocean resulting exclusively from nuclear weapons test fallout, which is 2.5×10^7 atoms·kg^{-1} (He et al., 2013). Furthermore, Fig. 5 shows that the inventory, 3.4×10^{14} atoms·m^{-2}, is comparable to those from station 1 and El-b, close to the British Islands and to a small extent affected by the releases from Sellafield. This may indicate a direct contribution from the liquid discharges from Sellafield and La Hague to the PAP site. Therefore, a small part of the liquid discharges from the NFRPs could be being advected to the South-West, directly affecting the North Atlantic Ocean, and not exclusively to the Nordic Seas. This would be in agreement with the results from a Lagrangian model which simulates the dispersion of ^{137}Cs (Periáñez et al., 2016) and ^{129}I (Villa et al., 2015) in the North Atlantic and predicted that a small percentage of Sellafield discharges are transported south, to the Celtic Sea and subsequently to the English Channel and to the open North Atlantic Ocean.

However, the contribution of gaseous releases from the NFRP, with high concentrations of ^{129}I, has to be accounted for. We compare the ^{129}I inventory at the PAP site with the inventories calculated in the Western and Eastern Mediterranean Sea, that ranged from 1 to 2.1×10^{14} atoms·m^{-2} and from 0.8 to 2.8×10^{14} atoms·m^{-2}, respectively (Castrillejo et al., 2017). The inventory at the PAP site is significantly higher, with uncertainties lower than 10% in this case. Castrillejo et al. (2017) simulated the trajectories of gaseous ^{129}I from Sellafield, La Hague and Marcoule in Europe and the Atlantic Ocean and the Mediterranean Sea. According to Castrillejo et al. (2017), ^{129}I concentrations at the Western Mediterranean are mostly influenced by gaseous releases from the French Marcoule NFRP, either directly or from washout from land. Furthermore, the contribution of gaseous releases from Sellafield to the ^{129}I inventory at the PAP site is negligible, but a certain contribution from La Hague is to be expected. Further data would be needed to determine if the higher inventories found at the PAP site correspond mainly to liquid discharges from the NFRP or are more affected by their gaseous contributions, mainly from La Hague.

4. Conclusions

^{129}I concentrations in the Nordic Seas in 2012 are at 10^9 atoms·kg^{-1} levels, because of the strong influence of the liquid discharges from Sellafield and La Hague, and in the North Atlantic at 10^8 atoms·kg^{-1} levels. ^{129}I concentrations have risen due to the increase in the releases from the NFRP that started during years 1990–1993 and reached a maximum in 1998.

Table 3
^{129}I concentrations in the Irish Sea, the Celtic Sea and in the PAP site.

Station	Latitude (°N)	Longitude (°E)	Bottom depth (m)	Depth (m)	^{129}I concentration (10^8 atoms·kg^{-1})	3σ (10^8 atoms·kg^{-1})
Ballycastle	55.21	−6.23		0	576	44
Ards	54.48	−5.60		0	1580	130
Woodstown	51.64	−9.91		0	18.01	0.90
Central Irish Sea	53.93	−5.11		0	1.271	0.022
Celtic Sea	50.50	−7.56		0	7.65	0.12
PAP	48.90	−16.27	4870	0	1.092	0.027
				30	1.323	0.054
				210	1.129	0.050
				500	1.053	0.045
				950	0.984	0.019
				3013	0.598	0.017
				4000	0.328	0.023
				4713	0.452	0.039

^{129}I concentrations and inventories in the North Atlantic Ocean, south-west of the British Isles suggest a direct impact of the NFRPs in that area, i.e. not 100% of the releases heads north bound into the NCC. This is in agreement with previous numerical models, but further analysis including consideration of contributions for gaseous discharges of ^{129}I is required.

The structure of the ^{129}I depth profiles in the Nordic Seas reveals the marine current patterns. T-S diagrams and iodine concentrations point out a possible deep-water formation in the Greenland Sea Gyre. This deep water spreads into the Norwegian Sea and overflows through the Denmark Strait. The inventories combined with the ^{129}I concentrations above and below 200 m support the conclusions from the T-S diagrams and delimit the location of the deep water formation. We believe that in year 2012 the formation covered the easternmost longitudes of the Nordic Seas, in both the Greenland Sea and the Norwegian Sea.

Further ^{129}I analysis, in cruises specifically outlined for these purposes, should be performed in order to better define the places where the deep-water formation takes place. This will complement the use of effective techniques such as Argos, to calculate volume, heat and freshwater budgets for the Arctic.

Acknowledgements

This work has been partially financed by the project FIS2015-69673-P by the Spanish Ministerio de Economía y Competitividad.

References

Alfimov, V., Aldahan, A., Possnert, G., 2004a. Tracing water masses with ^{129}I in the western Nordic Seas in early spring 2002. Geophys. Res. Lett. 31, L19305. https://doi.org/10.1029/2004GL020863.

Alfimov, V., Aldahan, A., Possnert, G., Kekli, A., Meili, M., 2004b. Concentrations of ^{129}I along a transect from the North Atlantic to the Baltic Sea. Nucl. Instruments Methods Phys. Res. Sect. B Beam Interact. with Mater. Atoms 223–224:446–450. https://doi.org/10.1016/j.nimb.2004.04.084.

Alfimov, V., Aldahan, A., Possnert, G., Winsor, P., 2004c. Anthropogenic iodine-129 in seawater along a transect from the Norwegian coastal current to the north pole. Mar. Pollut. Bull. 49:1097–1104. https://doi.org/10.1016/j.marpolbul.2004.08.019.

Alfimov, V., Possnert, G., Aldahan, A., 2006. Anthropogenic iodine-129 in the Arctic Ocean and Nordic Seas: numerical modeling and prognoses. Mar. Pollut. Bull. 52:380–385. https://doi.org/10.1016/j.marpolbul.2005.09.025.

Alfimov, V., Aldahan, A., Possnert, G., 2013. Water masses and ^{129}I distribution in the Nordic Seas. Nucl. Instruments Methods Phys. Res. Sect. B Beam Interact. with Mater. Atoms 294:542–546. https://doi.org/10.1016/j.nimb.2012.07.042.

AREVA, 2013. Cumulative release results report for the AREVA La Hague plant [WWW Document]. URL. http://www.new.areva.com/EN/operations-2315/cumulative-release-results-report-for-the-areva-la-hague-plant.html.

Bacon, S., 1998. Decadal variability in the outflow from the Nordic seas to the deep Atlantic Ocean. Nature 394:871–874. https://doi.org/10.1038/29736.

Buraglio, N., Aldahan, A.A., Possnert, G., 1999. Distribution and inventory of ^{129}I in the central Arctic Ocean. Geophys. Res. Lett. 26:1011–1014. https://doi.org/10.1029/1999GL900178.

Casacuberta, N., Masqué, P., Henderson, G., Rutgers van-der-Loeff, M., Bauch, D., Vockenhuber, C., Daraoui, A., Walther, C., Synal, H.-A., Christl, M., 2016. First ^{236}U data from the Arctic Ocean and use of ^{236}U/^{238}U and ^{129}I/^{236}U as a new dual tracer. Earth Planet. Sci. Lett. 440:127–134. https://doi.org/10.1016/j.epsl.2016.02.020.

Castrillejo, M., Casacuberta, N., Christl, M., Garcia-Orellana, J., Vockenhuber, C., Synal, H.-A., Masqué, P., 2017. Anthropogenic ^{236}U and ^{129}I in the Mediterranean Sea: first comprehensive distribution and constrain of their sources. Sci. Total Environ. 593–594:745–759. https://doi.org/10.1016/j.scitotenv.2017.03.201.

Christl, M., Casacuberta, N., Vockenhuber, C., Elsässer, C., Bailly du Bois, P., Herrmann, J., Synal, H.-A., 2015. Reconstruction of the ^{236}U input function for the Northeast Atlantic Ocean: implications for ^{129}I/^{236}U and ^{236}U/^{238}U-based tracer ages. J. Geophys. Res. Oceans 120:7282–7299. https://doi.org/10.1002/2015JC011116.

Daraoui, A., Riebe, B., Walther, C., Wershofen, H., Schlosser, C., Vockenhuber, C., Synal, H.-A., 2016. Concentrations of iodine isotopes (^{129}I and ^{127}I) and their isotopic ratios in aerosol samples from northern Germany. J. Environ. Radioact. 154:101–108. https://doi.org/10.1016/j.jenvrad.2016.01.021.

Dickson, R.R., Brown, J., 1994. The production of North Atlantic deep water: sources, rates, and pathways. J. Geophys. Res. Oceans 99:12319–12341. https://doi.org/10.1029/94JC00530.

Edmonds, H.N., Smith, J.N., Livingston, H.D., Kilius, L.R., Edmond, J.M., 1998. ^{129}I in archived seawater samples. Deep-Sea Res. I Oceanogr. Res. Pap. 45:1111–1125. https://doi.org/10.1016/S0967-0637(98)00007-7.

Fabryka-Martin, J., Davis, S.N., Elmore, D., 1987. Applications of ^{129}I and ^{36}Cl in hydrology. Nucl. Instruments Methods Phys. Res. Sect. B Beam Interact. with Mater. Atoms 29:361–371. https://doi.org/10.1016/0168-583X(87)90265-5.

Fan, Y., Hou, X., Zhou, W., 2013. Progress on ^{129}I analysis and its application in environmental and geological researches. Desalination 321:32–46. https://doi.org/10.1016/j.desal.2012.05.012.

Fehn, U., Holdren, G.R., Elmore, D., Brunelle, T., Teng, R., Kubik, P.W., 1986. Determination of natural and anthropogenic 129I in marine sediments. Geophys. Res. Lett. 13:137–139. https://doi.org/10.1029/GL013i002p00137.

Fogelqvist, E., Blindheim, J., Tanhua, T., Østerhus, S., Buch, E., Rey, F., 2003. Greenland–Scotland overflow studied by hydro-chemical multivariate analysis. Deep-Sea Res. I Oceanogr. Res. Pap. 50:73–102. https://doi.org/10.1016/S0967-0637(02)00131-0.

Gómez-Guzmán, J.M., López-Gutiérrez, J.M., Pinto-Gómez, A.R., Holm, E., 2012. ^{129}I measurements on the 1 MV AMS facility at the Centro Nacional de Aceleradores (CNA, Spain). Appl. Radiat. Isot. 70:263–268. https://doi.org/10.1016/j.apradiso.2011.07.018.

Gómez-Guzmán, J.M., Villa, M., Le Moigne, F., López-Gutiérrez, J.M., García-León, M., 2013. AMS measurements of ^{129}I in seawater around Iceland and the Irminger Sea. Nucl. Instruments Methods Phys. Res. Sect. B Beam Interact. with Mater. Atoms 294:547–551. https://doi.org/10.1016/j.nimb.2012.07.045.

Hansen, B., Østerhus, S., 2000. North Atlantic–Nordic Seas exchanges. Prog. Oceanogr. 45:109–208. https://doi.org/10.1016/S0079-6611(99)00052-X.

He, P., Aldahan, A., Possnert, G., Hou, X.L., 2013. A summary of global ^{129}I in marine waters. Nucl. Instruments Methods Phys. Res. Sect. B Beam Interact. with Mater. Atoms 294:537–541. https://doi.org/10.1016/j.nimb.2012.08.036.

Holliday, N.P., Waniek, J.J., Davidson, R., Wilson, D., Brown, L., Sanders, R., Pollard, R.T., Allen, J.T., 2006. Large-scale physical controls on phytoplankton growth in the Irminger Sea part I: hydrographic zones, mixing and stratification. J. Mar. Syst. 59:201–218. https://doi.org/10.1016/j.jmarsys.2005.10.004.

Huang, R.X., 2010. Ocean circulation: Wind-driven and Thermohaline Processes. Cambridge University Press.

IAEA, 2005. Status and Trends in Spent Fuel Reprocessing, IAEA-TECDOC-1467.

Jeansson, E., Jutterström, S., Rudels, B., Anderson, L.G., Anders Olsson, K., Jones, E.P., Smethie, W.M., Swift, J.H., 2008. Sources to the East Greenland current and its contribution to the Denmark Strait Overflow. Prog. Oceanogr. 78:12–28. https://doi.org/10.1016/j.pocean.2007.08.031.

Karcher, M., Smith, J.N., Kauker, F., Gerdes, R., Smethie, W.M., 2012. Recent changes in Arctic Ocean circulation revealed by iodine-129 observations and modeling. J. Geophys. Res. Oceans 117. https://doi.org/10.1029/2011JC007513 (n/a-n/a).

Lacan, F., Jeandel, C., 2004. Denmark Strait water circulation traced by heterogeneity in neodymium isotopic compositions. Deep-Sea Res. I Oceanogr. Res. Pap. 51:71–82. https://doi.org/10.1016/j.dsr.2003.09.006.

Latarius, K., Quadfasel, D., 2016. Water mass transformation in the deep basins of the Nordic Seas: analyses of heat and freshwater budgets. Deep-Sea Res. I Oceanogr. Res. Pap. 114:23–42. https://doi.org/10.1016/j.dsr.2016.04.012.

Logemann, K., Harms, I., 2006. High resolution modelling of the North Icelandic Irminger current (NIIC). Ocean Sci. 2:291–304. https://doi.org/10.5194/os-2-291-2006.

López-Gutiérrez, J.M., Synal, H.-A., Suter, M., Schnabel, C., Garćia-León, M., 2000. Accelerator mass spectrometry as a powerful tool for the determination of ^{129}I in rainwater. Appl. Radiat. Isot. 53:81–85. https://doi.org/10.1016/S0969-8043(00)00116-0.

López-Gutiérrez, J.M., García-León, M., Schnabel, C., Suter, M., Synal, H.-A., Szidat, S., García-Tenorio, R., 2004. Relative influence of ^{129}I sources in a sediment core from the Kattegat area. Sci. Total Environ. 323:195–210. https://doi.org/10.1016/j.scitotenv.2003.09.025.

Michel, R., Daraoui, A., Gorny, M., Jakob, D., Sachse, R., Tosch, L., Nies, H., Goroncy, I., Herrmann, J., Synal, H.A., Stocker, M., Alfimov, V., 2012. Iodine-129 and iodine-127 in European seawaters and in precipitation from Northern Germany. Sci. Total Environ. 419:151–169. https://doi.org/10.1016/j.scitotenv.2012.01.009.

Open University, 2001. Ocean Circulation. Butterworth Heinemann, Boston, US.

Orre, S., Smith, J.N., Alfimov, V., Bentsen, M., 2010. Simulating transport of ^{129}I and idealized tracers in the northern North Atlantic Ocean. Environ. Fluid Mech. 10:213–233. https://doi.org/10.1007/s10652-009-9138-3.

Periáñez, R., Suh, K.-S., Min, B.-I., 2016. The behaviour of ^{137}Cs in the North Atlantic Ocean assessed from numerical modelling: releases from nuclear fuel reprocessing factories, redissolution from contaminated sediments and leakage from dumped nuclear wastes. Mar. Pollut. Bull. 113:343–361. https://doi.org/10.1016/j.marpolbul.2016.10.021.

Pham, M.K., Betti, M., Povinec, P.P., Alfimov, V., Biddulph, D., Gastaud, J., Kieser, W.E., López Gutiérrez, J.M., Possnert, G., Sanchez-Cabeza, J.A., Suzuki, T., 2010. Certified reference material IAEA-418: ^{129}I in Mediterranean Sea water. J. Radioanal. Nucl. Chem. 286:121–127. https://doi.org/10.1007/s10967-010-0621-6.

Pickard, G.L., Emery, W.J., 1982. Descriptive Physical oceanography: An Introduction. Pergamon Press.

Rhein, M., Kieke, D., Hüttl-Kabus, S., Roessler, A., Mertens, C., Meissner, R., Klein, B., Böning, C.W., Yashayaev, I., 2011. Deep water formation, the subpolar gyre, and the meridional overturning circulation in the subpolar North Atlantic. Deep-Sea Res. II Top. Stud. Oceanogr. 58:1819–1832. https://doi.org/10.1016/j.dsr2.2010.10.061.

Sellafield Ltd., 2014. Annual discharge & monitoring reports [WWW Document]. URL. http://sustainability.sellafieldsites.com/environment/environment-page/annual-discharge-monitoring-reports/.

Smethie Jr., W.M., Fine, R.a., Putzka, A., Jones, E.P., 2000. Tracing the flow of North Atlantic Deep Water using chlorofluorocarbons. J. Geophys. Res. Oceans 105:14297–14323. https://doi.org/10.1029/1999JC900274.

Smith, J.N., Ellis, K.M., Kilius, L.R., 1998. ^{129}I and ^{137}Cs tracer measurements in the Arctic Ocean. Deep-Sea Res. I Oceanogr. Res. Pap. 45:959–984. https://doi.org/10.1016/S0967-0637(97)00107-6.

Smith, J.N., Jones, E.P., Moran, S.B., Smethie Jr., W.M., Kieser, W.E., 2005. Iodine 129/CFC 11 transit times for Denmark Strait Overflow Water in the Labrador and Irminger Seas. J. Geophys. Res. 110, C05006. https://doi.org/10.1029/2004JC002516.

Smith, J.N., McLaughlin, F.A., Smethie, W.M., Moran, S.B., Lepore, K., 2011. Iodine-129, ^{137}Cs, and CFC-11 tracer transit time distributions in the Arctic Ocean. J. Geophys. Res. 116, C04024. https://doi.org/10.1029/2010JC006471.

Tanhua, T., Olsson, K.A., Jeansson, E., 2005. Formation of Denmark Strait overflow water and its hydro-chemical composition. J. Mar. Syst. 57:264–288. https://doi.org/10.1016/j.jmarsys.2005.05.003.

Villa, M., López-Gutiérrez, J.M., Suh, K.-S., Min, B.-I., Periáñez, R., 2015. The behaviour of ^{129}I released from nuclear fuel reprocessing factories in the North Atlantic Ocean and transport to the Arctic assessed from numerical modelling. Mar. Pollut. Bull. 90:15–24. https://doi.org/10.1016/j.marpolbul.2014.11.039.

Waite, T.J., Truesdale, V.W., Olafsson, J., 2006. The distribution of dissolved inorganic iodine in the seas around Iceland. Mar. Chem. 101:54–67. https://doi.org/10.1016/j.marchem.2006.01.003.